

GravityGraphSAGE: Link Prediction in Directed Attributed Graphs

Riccardo Porcedda^{1,2}, Francesca Chiaromonte^{1,3}, Fabrizio Lillo⁴, Andrea Vandin^{1,5}

¹Department of Excellence L'EMbeDS, Sant'Anna School of Advanced Studies, Pisa, Italy

²Department of Computer Science, University of Pisa, Italy

³Department of Statistics and Huck Institutes of the Life Sciences, The Pennsylvania State University, USA

⁴Class of Science, Scuola Normale Superiore, Pisa, Italy

⁵DTU Technical University of Denmark, Lyngby, Denmark

Abstract

Link prediction (inferring missing or future connections between nodes in a graph) is a fundamental problem in network science with widespread applications in, e.g., biological systems, recommender systems, finance and cybersecurity. The ability to accurately predict links has significant real-world applications, such as detecting fraudulent financial transactions or identifying drug-target interactions in biomedicine. Despite a rich literature, link prediction is still challenging, especially for graphs enriched with information on edges (direction) and nodes (attributes). In fact, research on link prediction, especially the one based on Graph Deep Learning (GDL), has mostly focused on undirected graphs, without fully leveraging node attributes. Here, we fill this gap by proposing GravityGraphSAGE (GG-SAGE), a modified version of GraphSAGE, a GDL model for node embeddings, composed of a *gravity-inspired decoder*. This implementation is the first example in the literature of a GraphSAGE backbone adopted for directed link prediction. Using the benchmark datasets Cora, Citeseer, PubMed and 16 real-world graphs from the online Netzschleuder repository, we show that our proposed model outperforms state-of-the-art GDL link prediction techniques. Using further experimental evidence, we relate the quality of the output of our model with various characteristics of the graph, suggesting that our framework scales well when applied to data of increasing complexity.

Code — <https://doi.org/10.5281/zenodo.16722908>

1 Introduction

Link prediction in complex networks is the task of inferring potential or missing links (edges) between nodes based on intrinsic features of a network (Liben-Nowell and Kleinberg 2007). This problem has drawn extensive attention across fields, driven by its ubiquitous applications in social networks and biological systems (Almansoori et al. 2012), recommender systems (Huang, Li, and Chen 2005), finance (Spelta and Pecora 2023) and cybersecurity (Yin et al. 2023).

Traditional approaches for link prediction often rely on node similarity indices (Lü and Zhou 2011), such as common neighbors, Adamic-Adar, and preferential attachment, which use local or global topological features to estimate the likelihood of links between node pairs. These similarity-based methods, while intuitive and computationally feasible, are typically limited to undirected graphs and struggle with

more complex directed, attributed graphs. Moreover, they were outperformed by the introduction of Deep Learning methods for graph data, which led to Graph Deep Learning (Zhang, Cui, and Zhu 2022). The first proposals, where graph measures were used as input for basic neural networks (Zhang et al. 2016), were soon followed by the development of Graph Neural Networks (GNNs), which directly take as input networks represented through adjacency or laplacian matrices (Defferrard, Bresson, and Vandergheynst 2016). The general framework of GNNs for link prediction is the following (Zhang and Chen 2018): first, train the model to learn a low-dimensional vector representation for the nodes, i.e. an *embedding* (this can be done either in an unsupervised or in a supervised fashion); then, predict links by using a proximity measure (e.g., the inner product of two vectors) in the embedding space. However, and notably, most GNN advances to date concern undirected networks without attributes on nodes.

Contribution. In this work, we fill this gap by proposing a GNN approach for link prediction in directed, attributed graphs. Our proposal consists of combining a variant of GraphSAGE equipped with an ELU activation function on the final embedding layer, with a *gravity-inspired decoder* that was first proposed in (Salha et al. 2019), but never applied to this architecture. The former component allows us to handle node attributes in large-scale networks, while the latter accounts for edge directionality. Using real-world graphs from the Netzschleuder online repository, we show that our proposal outperforms state-of-the-art link prediction techniques.

Synopsis. Section 2 introduces some taxonomy in order to better define node embeddings (what they are, how they are generated, which are the state-of-the-art models) and the challenges posed by directed graphs and link prediction in GDL. Section 3 provides details of our proposal, the GravityGraphSAGE model, outlining how it differs from prior work by combining the inductive power of GraphSAGE with the gravity-inspired decoder. Section 4 describes the experimental settings and compares our model with state-of-the-art GDL methods on directed and attributed graphs selected from the Netzschleuder repository (<https://networks.skewed.de/>). Finally, Section 5 provides final remarks and outlines directions for future research.

2 Preliminaries and related works

We now provide relevant preliminary material and highlight related works on which our method is based.

Directed, unweighted, and attributed graphs

Let $G(\mathcal{V}, \mathcal{E}, F)$ be a directed, unweighted and attributed graph, where \mathcal{V} represents the set of n nodes, $\mathcal{E} \subseteq \mathcal{V} \times \mathcal{V}$ is the set of m edges and $F \in \mathbb{R}^{n \times d}$ is the node attribute matrix with d being the number of features. An edge $e_{ij} \in \mathcal{E}$ connects node v_i to node v_j . A graph can also be compactly represented as an adjacency matrix A given as $A_{ij} = e_{ij}$ for all i, j . In the case of a directed and unweighted graph, this matrix is binary, $A_{ij} \in \{0, 1\}$. The shortest distance from node i to node j is the minimum number of edges that have to be crossed to get from i to j . As shown in Figure 1, the K -hop neighborhood $\mathcal{N}_K(v)$ of a node v is the set of nodes at distances at most K from that node.

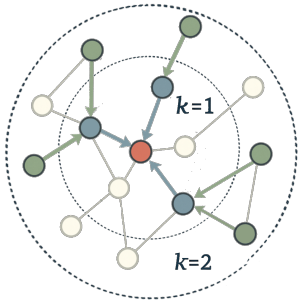


Figure 1: Example of K -hop neighborhood

In terms of adjacency matrix, we have $\mathcal{N}_K(v) = \{u | A_{uv}^K \neq 0\}$. If we consider the whole neighborhood, without posing a bound K on the distance, then we write $\mathcal{N}(v)$.

Node Embeddings

Node embeddings, i.e. low-dimensional vector representations of nodes in a graph, are a fundamental technique in graph-based machine learning and are employed in various downstream tasks, including node classification, link prediction, and clustering (Cai, Zheng, and Chang 2018). Traditional methods, such as matrix factorization (Belkin and Niyogi 2003; Ou et al. 2016), laid the groundwork for embedding techniques by decomposing adjacency or Laplacian matrices to capture latent relationships. However, these approaches faced challenges in scalability and flexibility. The advent of random walk-based methods, like DeepWalk (Perozzi, Al-Rfou, and Skiena 2014) and node2vec (Grover and Leskovec 2016), extended neural language models to graph structures to learn node representations, effectively capturing both local and global structural information. Notably though, it has been shown that these models, too, rely on some kind of matrix factorization (Levy and Goldberg 2014; Qiu et al. 2018).

Later, more complex GNNs have been developed to leverage both node attributes and topological information. The main idea shared by these models is, for each node, to aggregate the features of its neighbors and combine them to

Model	Description
GCN	<p>Key Idea: Aggregates and averages neighbor features via message passing</p> <p>Strengths: Efficient due to sparse matrix multiplication</p> <p>Weaknesses: Assigns equal importance to all neighbors; requires full adjacency matrix, limiting scalability</p>
GAT	<p>Key Idea: Uses <i>self-attention</i> to assign adaptive weights to neighboring nodes</p> <p>Strengths: Can learn specific importance of neighbors</p> <p>Weaknesses: Computationally expensive due to pairwise attention computations; requires full adjacency matrix</p>
GraphSAGE	<p>Key Idea: Uses <i>sampling</i> to aggregate neighborhood information instead of full adjacency matrix</p> <p>Strengths: Can generalize to unseen nodes; it does not require full graph storage; better handles oversmoothing</p> <p>Weaknesses: Sampling introduces stochasticity in training; ignores <i>distant neighbors</i> beyond sampled depth</p>

Table 1: Comparison of main GNN architectures

the features of the node itself. This process is referred to as *message-passing* (Figure 2).

Message-passing can be implemented in different ways. The most popular utilize architectures such as Graph Convolutional Networks (GCN) (Kipf and Welling 2017), Graph Attention Networks (GAT) (Veličković et al. 2018) and GraphSAGE (Hamilton, Ying, and Leskovec 2018). The key features of these architectures are summarized in Table 1 and further discussed below.

From now on, let

- $h_v^{(l)} \in \mathbb{R}^{d_l}$ be the representation of node v at layer l ;
- $W^{(l)} \in \mathbb{R}^{d_{l-1} \times d_l}$ be the learnable weight matrix; and
- $f^{(k)}$ be an activation function (e.g., ReLU).

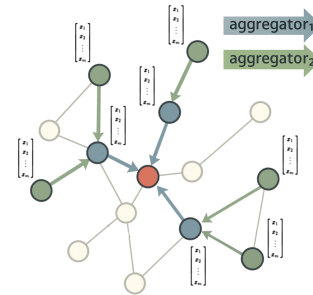


Figure 2: Example of message-passing

At layer $l = 0$ (the input), we have $h_v^{(0)} = F_v$, i.e. the original attributes of node v . Thus, defining $H^{(l)} = [h_1^{(l)} h_2^{(l)} \dots h_n^{(l)}] \in \mathbb{R}^{n \times d_l}$ for the entire graph, we have $H^{(0)} = F$. If no node attribute matrix is given, then we set $F = I$.

Graph Convolutional Networks (GCN). GCNs extend the concept of convolution from grid-like structures (e.g., images) to graphs. The message-passing form here is

$$h_v^{(l)} = f^{(l)} \left(W^{(l)} \cdot \frac{h_v^{(l-1)} + \sum_{u \in \mathcal{N}(v)} h_u^{(l-1)}}{1 + |\mathcal{N}(v)|} \right)$$

which can be rewritten more compactly as

$$H^{(l)} = f^{(l)}(D^{-1}AH^{(l)}W^{(l)})$$

where $D \in \mathbb{R}^{n \times n}$ is the diagonal node degree matrix.

The message-passing in GCNs is basically an average of the selected node representation $h_v^{(l-1)}$ and the aggregated (summed) representations of its neighborhood. This means that all neighbors are given equal importance, which may not always be appropriate. Furthermore, while the convolution operation in matrix form can leverage sparse matrix multiplication for scalability, it is important to note that GCNs require the entire adjacency matrix; this poses a challenge when scaling to large graphs.

Graph Attention Networks (GAT). GATs introduce *self-attention mechanisms* (Bahdanau 2014; Vaswani et al. 2023) to dynamically weigh neighbor contributions. The update rule here is

$$h_v^{(l)} = f^{(l)} \left(W^{(l)} \left[\sum_{u \in \mathcal{N}(v)} \alpha_{vu}^{(l-1)} h_u^{(l-1)} + \alpha_{vv}^{(l-1)} h_v^{(l-1)} \right] \right)$$

where α_{vu} is the *attention coefficient*, which represents the importance of neighbor u to node v .

The obvious advantage of this form of message-passing is that, unlike GCNs, it does not assign the same relevance to the whole neighborhood – thus allowing better aggregation and feature learning. The inevitable drawbacks are a larger number of parameters and an increased computational burden due to the pairwise attention coefficients α_{vu} .

GraphSAGE (Sample and Aggregate). GCNs and GATs require access to the full graph (the entire adjacency matrix) during training. Hence, if nodes are added to the graph, a new training is required; this is called *transductive learning*. In contrast, GraphSAGE is designed for *inductive learning*, meaning that it can leverage node attribute information to efficiently generate representations on previously unseen data. GraphSAGE’s uses a neighborhood sampling strategy through the update rule

$$h_v^{(l)} = f^{(l)} \left(W^{(l)} \left[\text{AGG}_{u \in \mathcal{N}_K(v)} \left(\{h_u^{(l-1)}\} \right), h_v^{(l-1)} \right] \right) \quad (1)$$

where the aggregation function can be averaging, LSTM-based, or pooling. In symbols, aggregation through averaging has the form

$$\text{AGG}_{u \in \mathcal{N}_K(v)} \left(\{h_u^{(l-1)}\} \right) = \frac{h_v^{(l-1)} + \sum_{u \in \mathcal{N}_K(v)} h_u^{(l-1)}}{1 + |\mathcal{N}_K(v)|}. \quad (2)$$

Note that this aggregation function leads to a message-passing rule similar to that of GCNs. However, before applying the transformation $W^{(k)}$, GraphSAGE concatenates the aggregated features of the neighborhood $\mathcal{N}_K(v)$ with the features of the node v . This avoids *oversmoothing* of node embeddings, i.e. excessively similar representations for different nodes. It has been shown that GraphSAGE, within the first three layers, tackles this problem better than GCNs and GATs (Chen et al. 2020). Since aggregation here is the result of a concatenation, for the weight matrix we trivially have $W \in \mathbb{R}^{2d_{l-1} \times d_l}$.

Link Prediction

Once embeddings have been obtained – say h_u and h_v for nodes u and v , respectively – the typical link prediction approach leverages their inner product. An edge is predicted as

$$A_{uv} = \sigma(h_u \cdot h_v)$$

where σ indicates the sigmoid function. However, this approach has the inherent drawback of lacking directionality; due to the symmetry of the inner product, the prediction is the same for in-edges and out-edges.

Directed Link Prediction. One way to overcome this drawback is the Source/Target Vector Paradigm (Zhou et al. 2017), where each node has two separate embeddings as a source and as a target. This allows one to use the inner product for a source/target pair of nodes, introducing asymmetry in the link prediction process:

$$A_{uv} = \sigma(h_u^{\text{source}} \cdot h_v^{\text{target}}).$$

A similar pathway involves using complex numbers (Zhang et al. 2021; Li et al. 2024), which still results in learning two vector representations for each node. While intuitive and straightforward, this paradigm at best doubles the number of parameters to be trained. A more elegant solution was found by including just one additional parameter to be learned in the embedding of each node; namely, its *mass* (Salha et al. 2019). This approach was inspired by Newtonian gravity, where the force felt by two bodies results in different accelerations due to the difference in their masses; in symbols

$$F = G \frac{m_1 m_2}{r^2} \quad a_{1 \rightarrow 2} = \frac{F}{m_1} = \frac{G m_2}{r^2}$$

where G is the gravitational constant, m_1, m_2 are the masses, r is the distance between those two. If one defines the embedding h_u of node u as

$$h_u = \left(\begin{array}{c} \bar{h}_u \\ \log(G m_u) \end{array} \right) = \left(\begin{array}{c} \bar{h}_u \\ \tilde{m}_u \end{array} \right)$$

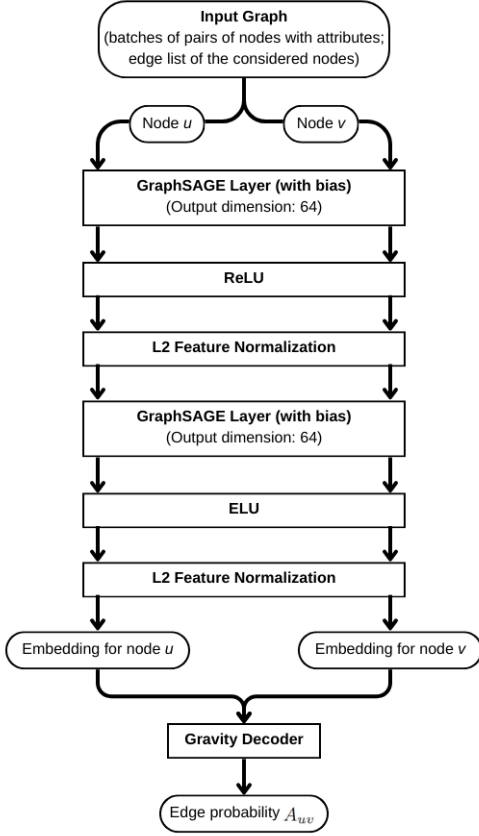


Figure 3: Schematic illustration of GG-SAGE

where \bar{h}_u can be interpreted as the position of mass m_u in the embedding space, the acceleration in Equation 2 can be rewritten, on the log scale, as

$$\begin{aligned} A_{uv} &= \log(a_{u \rightarrow v}) \\ &= \sigma(\log(Gm_v) - \log \|h_u - h_v\|^2) \\ &= \sigma(\tilde{m}_v - \log \|h_u - h_v\|^2). \end{aligned}$$

This asymmetric quantity is then used as a prompt for directed link prediction (the logarithm is used because, transforming ratios into differences, it makes computation more stable). Other examples of this approach include the use of a gravity decoder in a hyperbolic space (Zhou et al. 2023).

3 GravityGraphSAGE

So far we discussed state-of-the-art approaches for link prediction based on GNNs. In their original formulations, none of these approaches supported *directed* link prediction (Zhang and Chen 2018; Cai et al. 2022; Papadimitriou, Symeonidis, and Manolopoulos 2012; Wang et al. 2014; Pan, Shi, and Dokmanić 2021; Ucar 2023). However, proposals have been introduced to address this issue for two out of three of the architectures considered. For GCNs, Salha and colleagues (Salha et al. 2019) implemented a Graph AutoEncoder (GAE) and a Graph Variational AutoEncoder (VGAE).

They tested these architectures, first integrating them with their gravity-inspired decoder (Gravity GAE/VGAE) and then following the Source/Target Vector Paradigm (Source/Target GAE/VGAE). For GATs, there are examples in the literature employing the Source/Target Vector Paradigm (Feng et al. 2022; Ke et al. 2024). Notably though, no proposals exists in the literature to extend GraphSAGE with directed link prediction capabilities.

We fill this gap introducing GravityGraphSAGE (GG-SAGE), an extension of GraphSAGE for directed link prediction. As illustrated in Figure 3, GG-SAGE uses the gravity-inspired decoder discussed above. Furthermore, it comprises two message-passing layers based on the average aggregator described in Equation 2:

$$h_v^{(1)} = \text{ReLU} \left(W^{(1)} \left[\text{AGG}_{u \in \mathcal{N}(v)} \left(\{h_u^{(0)}\} \right), h_v^{(0)} \right] + b^{(1)} \right)$$

$$\tilde{h}_v^{(1)} = \frac{h_v^{(1)}}{\|h_v^{(1)}\|_2}$$

$$h_v^{(2)} = \text{ELU} \left(W^{(2)} \left[\text{AGG}_{u \in \mathcal{N}(v)} \left(\{\tilde{h}_u^{(1)}\} \right), \tilde{h}_v^{(1)} \right] + b^{(2)} \right)$$

$$\tilde{h}_v^{(2)} = \frac{h_v^{(2)}}{\|h_v^{(2)}\|_2}.$$

Comparing this model to the original GraphSAGE in Equation 1, some important choices and additions deserve a deeper discussion. First, we add a bias term $b^{(l)} \in \mathbb{R}^{d_l}$. Second, we apply an L2 feature normalization at each layer. This reduces oversmoothing and establishes a direct connection between node similarity and the Euclidean distance we adopt in the decoder (Yang, Meng, and King 2021). Third, we use ELU (Clevert 2015) as activation function for the final layer rather than ReLU. The ELU activation function has negative output values, a *desideratum* in this setting for two reasons:

- negative values push mean unit activations closer to zero, like batch normalization, but with lower computational complexity – this has been shown to speed up learning (Clevert 2015);
- negative values for the mass parameter allow the gravity-inspired decoder to account for repulsive effects between nodes.

In the next section we experimentally demonstrate that these components lead to a method for directed link prediction which outperforms state-of-the-art competitor techniques in terms of established metrics.

4 Experiments

In this section, we outline the experimental setup used to validate GG-SAGE, including details on the datasets, the implementation of the validated models, and their training configurations. We then analyze the results, providing insights into the relationship between model performance and graph properties.

Experimental setting

We run our experiments on a virtual machine with 40 Intel(R) Xeon(R) Gold 6252 CPUs (base frequency of 2.10 GHz) and 96 GB of RAM. We compare GG-SAGE with Gravity GAE/VGAE, Source/Target GAE/VGAE (Salha et al. 2019), LightDiC (Li et al. 2024) and D-HYPR (Zhou et al. 2023) (other above-mentioned models were not considered for experiments because they are either outperformed by the chosen ones or because the replicability material is absent or not functioning).

All models are implemented using PyTorch Geometric^{1,2}. The original implementations of Gravity GAE/VGAE and Source/Target GAE/VGAE were based on Tensorflow, but the authors also referenced a PyTorch version³ which we include in our replicability material. In order to ensure a fair comparison, all architectures are constructed with two message-passing layers, and with common parameters. In particular, we use hidden dimension $d_l = 64$ for both $l = 1$ and $l = 2$, and for the training routine we employ a learning rate of 0.001, 200 epochs with early stopping and a batch size of 128.

Task definition

In order to evaluate the models we perform a 5-fold cross validation with resampling. In each iteration, we split training, validation and test set as follows. As training set we use incomplete versions of a graph where 15% of the edges are randomly removed accounting for directionality (if an edge between nodes u and v is reciprocal, we may remove the edge (u, v) while still retaining its reverse counterpart (v, u) in the training graph). Furthermore, as commonly done in the literature (Zhang and Chen 2018; Cai et al. 2022; Papadimitriou, Symeonidis, and Manolopoulos 2012; Wang et al. 2014; Pan, Shi, and Dokmanić 2021; Ucar 2023; Salha et al. 2019), we pair edges with an equal number of randomly sampled non-existent edges (i.e., pairs of nodes that were not originally connected). This is commonly known as *negative sampling* (Yang et al. 2020). Validation and test sets are built using the edges removed from the training set; specifically 5% are assigned to validation and 10% to testing. Again, as done for the training set and in line with the literature, we add negative samples to both validation and test sets. The validation set is used exclusively for early stopping to optimize model performance.

The performance of a model is evaluated on a binary classification task, where each pair of nodes has label 1 if connected by an edge, and 0 otherwise.

Following the literature (Zhang and Chen 2018; Cai et al. 2022; Papadimitriou, Symeonidis, and Manolopoulos 2012; Wang et al. 2014; Pan, Shi, and Dokmanić 2021; Ucar 2023; Salha et al. 2019), we use the AUC (Area Under the ROC Curve) and AP (Average Precision, the area under the precision-recall curve) as evaluation metrics. AUC measures the probability that a randomly chosen positive example (a real edge) is ranked higher than a randomly chosen negative

example (a non-existent edge). Instead, AP focuses on performance for the positive class (edges that exist). These are the two most employed metrics for classification tasks, since they are *threshold-independent* (unlike accuracy, they do not require choosing a classification threshold).

Datasets

For a first quick evaluation, we use the well-known Cora, Citeseer and PubMed datasets. Later on, to ensure a broad, domain-agnostic benchmarking and for the purpose of our ablation study in Section 4, we use the Netzschleuder repository (<https://networks.skewed.de/>). This public online repository contains 286 datasets, for a total of 163 735 networks, of which 71 426 undirected, 92 309 directed, and 8 490 bipartite. Among the directed graphs, 89 307 have attributes on nodes. We consider all graphs as unweighted, that is, we set the weight to 1 for all edges. For computational feasibility, we restrict attention to (directed, attributed) graphs containing between 150 and 20 000 nodes, and no more than 200 000 edges. These are listed in Table 1 of the Supplementary Material. We note that the cora-1998 dataset available in the Netzschleuder repository is not the same as the above-mentioned Cora dataset broadly used in the literature (Cai et al. 2022; Salha et al. 2019; Ucar 2023).

To select and download the datasets, we used EasyNetz⁴, a Python tool that allows the user to easily specify criteria such as whether the graphs are directed, undirected, weighted, unweighted, and various properties like the number of nodes, edges, etc. Once the graphs are filtered according to the criteria, they can be downloaded and exported into CSV files.

Results

Table 2 and figures 4 and 5 show the results of our experiments in terms of AUC and AP, respectively. For each dataset (row in the figures), we report the metrics as computed for each method. Datasets are sorted from top to bottom in order of decreasing size (number of edges), and datasets on which GG-SAGE achieves state-of-the-art performance are highlighted in green. In these cases (3 out of 3 for Cora, Citeseer and PubMed; 9 out of 16 Netzschleuder datasets for AUC and 10 for AP) our proposal performs best, or on par with the best performing among the considered competitors (i.e. with statistically undistinguishable metrics).

It is evident that GG-SAGE works best on large graphs, where it is by far the best method, with the exception of the *google* and *cora-1998* datasets, where the best model is LightDiC. There are four datasets in which LightDiC, D-HYPR and Source/Target GAE outperform by far the other models (*foodweb_little_rock*, *messal_shale*, *faculty_hiring*, *advogato*) and one in which it yields performances similar to GG-SAGE (*faculty_hiring_us*). Notably these datasets, which represent food webs, trust networks, or academic flow networks, are all hierarchical. Future work may investigate why these models better handle this type of relationships in a graph.

In Table 2 of the Supplementary Material, we report the complete numerical results for the Netzschleuder datasets,

¹LightDiC: <https://github.com/xkLi-Allen/LightDiC>

²D-HYPR: <https://github.com/hongluzhou/dhypr>

³https://github.com/ClaudMor/gravity_gae_torch_geometric

⁴<https://doi.org/10.5281/zenodo.14710814>

	Model	AUC (%)	AP (%)
Citeseer	GG-SAGE	88.90 ± 1.56	88.93 ± 1.57
	Gravity GAE	72.57 ± 0.49	80.98 ± 0.29
	Gravity VGAE	59.28 ± 1.54	66.22 ± 1.08
	S/T GAE	76.06 ± 0.69	81.94 ± 0.72
	S/T VGAE	69.84 ± 9.54	71.92 ± 10.48
	LightDiC	86.10 ± 0.30	79.70 ± 0.20
	D-HYPR	85.52 ± 1.13	86.34 ± 1.19
Cora	GG-SAGE	93.61 ± 1.82	93.69 ± 1.79
	Gravity GAE	85.04 ± 0.19	88.57 ± 0.33
	Gravity VGAE	56.28 ± 0.28	62.81 ± 0.55
	S/T GAE	82.67 ± 0.69	85.53 ± 0.79
	S/T VGAE	75.90 ± 1.14	77.20 ± 1.45
	LightDiC	86.10 ± 0.30	80.50 ± 0.20
	D-HYPR	88.22 ± 1.21	85.36 ± 1.34
Pubmed	GG-SAGE	81.05 ± 1.48	80.80 ± 1.13
	Gravity GAE	76.17 ± 0.28	82.53 ± 0.13
	Gravity VGAE	66.78 ± 0.36	70.53 ± 0.19
	S/T GAE	69.80 ± 0.19	73.67 ± 0.37
	S/T VGAE	66.20 ± 0.30	68.34 ± 0.50
	LightDiC	79.50 ± 0.20	73.20 ± 0.20
	D-HYPR	79.03 ± 1.21	79.81 ± 1.24

Table 2: AUC and AP results (%) for Cora, Citeseer and Pubmed datasets. Best results are highlighted in green and in bold are indicated comparable performances.

highlighting in green the best-performing model.

Relation between performance and graph properties

Another relevant question is how basic graph properties (number of nodes, edges and node features) influence the performance of the considered models. To address this, we use a Random Forest Regression to regress performance metrics on graph properties. Fit results are shown in Tables 3 and 4.

AUC – Random-Forest Fit				
Model	R ²	Feature importance		
		#Nodes	#Edges	#Features
GG-SAGE	0.849	<u>0.387</u>	0.439	0.174
Gravity GAE	0.915	0.099	<u>0.238</u>	0.663
Gravity VGAE	0.905	0.104	<u>0.244</u>	0.652
S/T GAE	0.849	<u>0.386</u>	0.146	0.468
S/T VGAE	0.827	<u>0.230</u>	<u>0.275</u>	0.496
LightDiC	0.826	0.270	<u>0.315</u>	0.415
D-HYPR	0.825	0.278	<u>0.319</u>	0.403

Table 3: Random-Forest R^2 and feature importances for predicting AUC. In bold, the relative importance of the most informative feature. Underlined, the second most informative.

For all models, the R^2 is above 85%, hence these three variables already give a reliable, though not exhaustive, description of their behaviour.

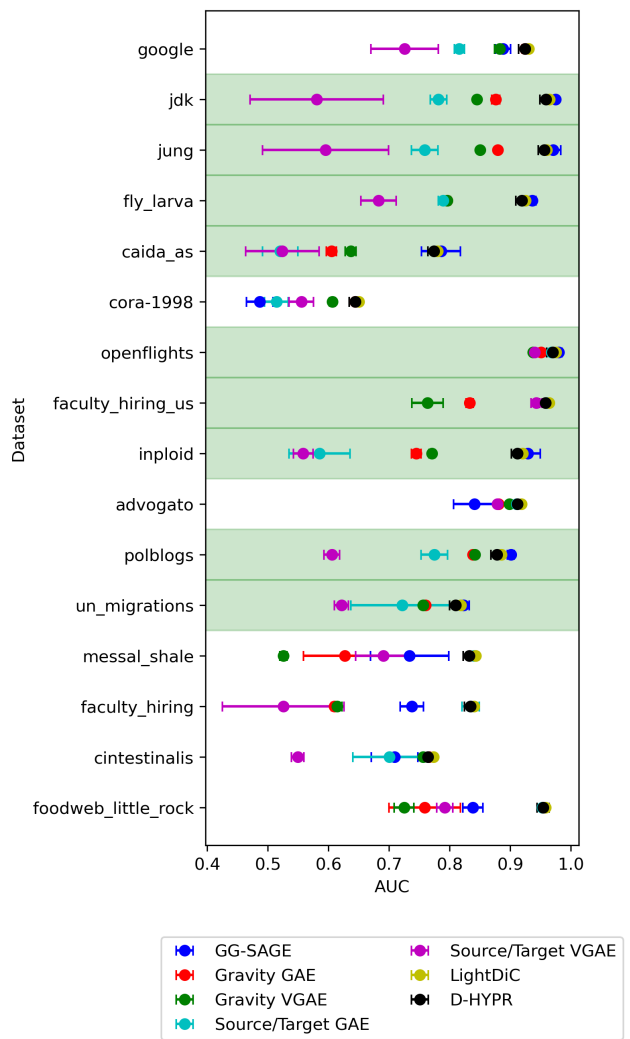


Figure 4: AUC of compared models across Netzschleuder selected datasets

One-way partial dependencies. In Figures 1-3 of the Supplementary Material, we visualize the marginal effect of each variable on the surrogate predictions. Across all methods larger edge sets correlate with higher accuracy, but the slopes differ markedly: GG-SAGE rises fastest (we notice an increment of 14% in AUC and AP before saturating near $5 \cdot 10^5$ edges, whereas Gravity GAE/VGAE and Source/Target GAE/VGAE gain only 7%–10%, while LightDiC and D-HYPR improve modestly because they already start from a high baseline). The dependence on the number of node features is almost flat for GG-SAGE but approximately linear for the Gravity GAE/VGAE and Source/Target GAE/VGAE, which obtain up to +13% AP when the number of features grows to 10 000, reaching then a plateau. With respect to the number of nodes, GG-SAGE, LightDiC and D-HYPR display a shallow peak around 4 000 nodes followed by a gradual decline, while the Gravity GAE/VGAE remain essentially level and the Source/Target variants deteriorate on large graphs.

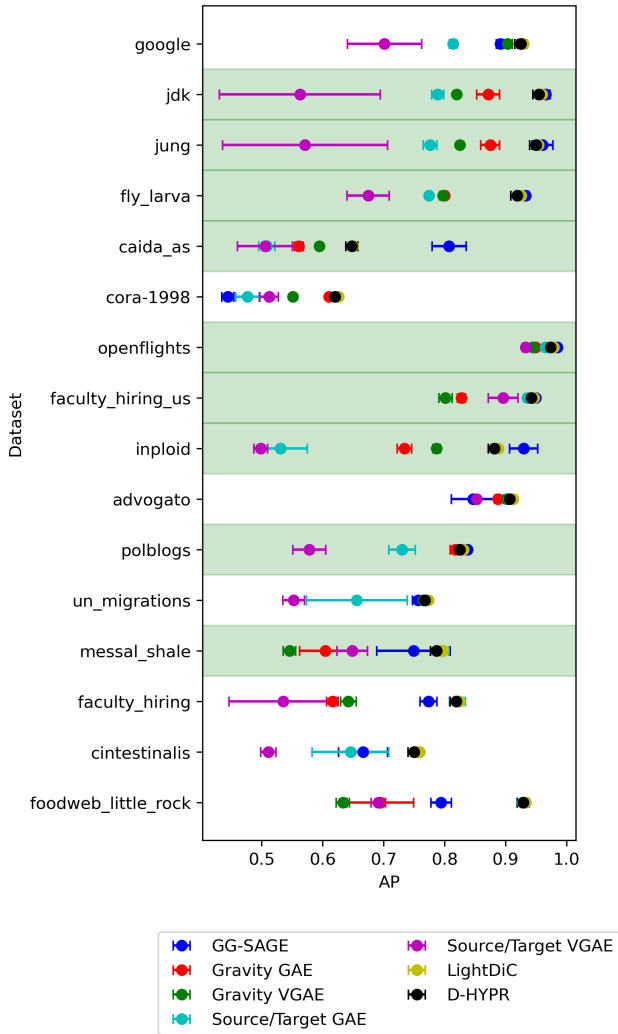


Figure 5: AP of compared models across Netzschleuder selected datasets

Discussion. Taken together, the surrogate study confirms that GG-SAGE derives its predictive power primarily from topological cues—particularly edge density—while remaining largely insensitive to the variation of node attributes, but still maintaining high performances. All competitor models, in contrast, are feature-driven and therefore benefit strongly from high-dimensional attributes, and LightDiC as well as D-HYPR occupy a middle ground with balanced reliance on structure and attributes. GG-SAGE’s edge-dominated response makes it comparatively robust in scenarios where structural information is available but rich node features are sparse or noisy.

5 Conclusions

In this paper, we proposed GravityGraphSAGE (GG-SAGE), a novel approach for directed link prediction in directed attributed graphs. GraphSAGE is a popular graph neural network model, able to perform several tasks, which is known to

AP – Random-Forest Fit				
Model	R^2	Feature importance		
		#Nodes	#Edges	#Features
GG-SAGE	0.855	<u>0.425</u>	0.479	0.095
Gravity GAE	0.917	0.111	<u>0.269</u>	0.620
Gravity VGAE	0.893	0.136	<u>0.312</u>	0.552
S/T GAE	0.848	<u>0.333</u>	0.141	0.526
S/T VGAE	0.854	0.218	<u>0.248</u>	0.534
LightDiC	0.878	0.197	<u>0.323</u>	0.481
D-HYPR	0.882	0.180	<u>0.318</u>	0.502

Table 4: Random-Forest R^2 and feature importances for predicting AP. Bold and underlined have the same meaning as in Table 3.

effectively use information on node attributes in large graphs. GG-SAGE integrates a customized GraphSAGE backbone with a gravity-inspired decoder. To the best of our knowledge, ours is the first GraphSAGE-based approach developed for directed link prediction.

We evaluated GG-SAGE against state-of-the-art methods for directed link prediction (LightDiC, D-HYPR, Gravity GAE/VGAE and Source/Target GAE/VGAE) on three well-known datasets (Cora, Citeseer and PubMed) and 16 real-world directed and attributed graphs from the public online repository Netzschleuder. The results demonstrate that GG-SAGE consistently outperforms, or matches, the best existing methods, particularly excelling in large-scale networks.

Through a Random Forest Regression, we showed that GG-SAGE uniquely benefits from increased graph connectivity (edge density), counteracting the performance degradation observed for all methods as the number of nodes increases. This suggests that our method is particularly suited for large, well-connected graphs.

Future Work. Our study raises several interesting directions for future research. First, as discussed in Section 4, it is of interest to investigate why the Source/Target Vector Paradigm, LightDiC and D-HYPR excel in hierarchical networks. Another interesting aspect to investigate is the impact of the negative sampling applied to datasets, in particular to the test set, commonly performed in the literature. Lastly, it is of interest to explore how improved performance in directed link prediction, such as the one afforded by GG-SAGE, may benefit richer pipelines which include this step.

References

- Almansoori, W.; Gao, S.; Jarada, T. N.; Elsheikh, A. M.; Murshed, A. N.; Jida, J.; Alhadj, R.; and Rokne, J. 2012. Link prediction and classification in social networks and its application in healthcare and systems biology. *Network Modeling Analysis in Health Informatics and Bioinformatics*, 1: 27–36.
- Bahdanau, D. 2014. Neural machine translation by jointly learning to align and translate. *arXiv preprint arXiv:1409.0473*.

- Belkin, M.; and Niyogi, P. 2003. Laplacian Eigenmaps for Dimensionality Reduction and Data Representation. *Neural Computation*, 15(6): 1373–1396.
- Cai, H.; Zheng, V. W.; and Chang, K. C.-C. 2018. A Comprehensive Survey of Graph Embedding: Problems, Techniques, and Applications. *IEEE Transactions on Knowledge & Data Engineering*, 30(09): 1616–1637.
- Cai, L.; Li, J.; Wang, J.; and Ji, S. 2022. Line Graph Neural Networks for Link Prediction. *IEEE Transactions on Pattern Analysis and Machine Intelligence*, 44(9): 5103–5113.
- Chen, D.; Lin, Y.; Li, W.; Li, P.; Zhou, J.; and Sun, X. 2020. Measuring and Relieving the Over-Smoothing Problem for Graph Neural Networks from the Topological View. *Proceedings of the AAAI Conference on Artificial Intelligence*, 34(04): 3438–3445.
- Clevert, D.-A. 2015. Fast and accurate deep network learning by exponential linear units (elus). *arXiv preprint arXiv:1511.07289*.
- Defferrard, M.; Bresson, X.; and Vandergheynst, P. 2016. Convolutional Neural Networks on Graphs with Fast Localized Spectral Filtering. *CoRR*, abs/1606.09375.
- Feng, Y.-Y.; Yu, H.; Feng, Y.-H.; and Shi, J.-Y. 2022. Directed graph attention networks for predicting asymmetric drug–drug interactions. *Briefings in Bioinformatics*, 23(3): bbac151.
- Grover, A.; and Leskovec, J. 2016. node2vec: Scalable Feature Learning for Networks. *arXiv:1607.00653*.
- Hamilton, W. L.; Ying, R.; and Leskovec, J. 2018. Inductive Representation Learning on Large Graphs. *arXiv:1706.02216*.
- Huang, Z.; Li, X.; and Chen, H. 2005. Link prediction approach to collaborative filtering. In *Proceedings of the 5th ACM/IEEE-CS Joint Conference on Digital Libraries*, JCDL '05, 141–142. New York, NY, USA: Association for Computing Machinery. ISBN 1581138768.
- Ke, Z.; Yu, H.; Li, J.; and Zhang, H. 2024. DUPLEX: dual GAT for complex embedding of directed graphs. In *Proceedings of the 41st International Conference on Machine Learning*, ICML'24. JMLR.org.
- Kipf, T. N.; and Welling, M. 2017. Semi-Supervised Classification with Graph Convolutional Networks. In *International Conference on Learning Representations*.
- Levy, O.; and Goldberg, Y. 2014. Neural Word Embedding as Implicit Matrix Factorization. In Ghahramani, Z.; Welling, M.; Cortes, C.; Lawrence, N.; and Weinberger, K., eds., *Advances in Neural Information Processing Systems*, volume 27. Curran Associates, Inc.
- Li, X.; Liao, M.; Wu, Z.; Su, D.; Zhang, W.; Li, R.-H.; and Wang, G. 2024. LightDiC: A Simple Yet Effective Approach for Large-Scale Digraph Representation Learning. *Proc. VLDB Endow.*, 17(7): 1542–1551.
- Liben-Nowell, D.; and Kleinberg, J. 2007. The link-prediction problem for social networks. *Journal of the American Society for Information Science and Technology*, 58(7): 1019–1031.
- Lü, L.; and Zhou, T. 2011. Link prediction in complex networks: A survey. *Physica A: Statistical Mechanics and its Applications*, 390(6): 1150–1170.
- Ou, M.; Cui, P.; Pei, J.; Zhang, Z.; and Zhu, W. 2016. Asymmetric Transitivity Preserving Graph Embedding. In *Proceedings of 22nd KDD*, KDD '16, 1105–1114. New York, NY, USA: ACM. ISBN 9781450342322.
- Pan, L.; Shi, C.; and Dokmanić, I. 2021. Neural Link Prediction with Walk Pooling. *arXiv preprint arXiv:2110.04375*.
- Papadimitriou, A.; Symeonidis, P.; and Manolopoulos, Y. 2012. Fast and accurate link prediction in social networking systems. *Journal of Systems and Software*, 85(9): 2119–2132. Selected papers from the 2011 Joint Working IEEE/IFIP Conference on Software Architecture (WICSA 2011).
- Perozzi, B.; Al-Rfou, R.; and Skiena, S. 2014. DeepWalk: on-line learning of social representations. In *Proceedings of the 20th ACM SIGKDD international conference on Knowledge discovery and data mining*, KDD '14, 701–710. ACM.
- Qiu, J.; Dong, Y.; Ma, H.; Li, J.; Wang, K.; and Tang, J. 2018. Network Embedding as Matrix Factorization: Unifying DeepWalk, LINE, PTE, and node2vec. In *Proceedings of the Eleventh ACM International Conference on Web Search and Data Mining*, WSDM '18, 459–467. New York, NY, USA: Association for Computing Machinery. ISBN 9781450355810.
- Salha, G.; Limnios, S.; Hennequin, R.; Tran, V.-A.; and Vazirgiannis, M. 2019. Gravity-Inspired Graph Autoencoders for Directed Link Prediction. In *Proceedings of the 28th CIKM*, 589–598. New York, NY, USA: ACM. ISBN 9781450369763.
- Spelta, A.; and Pecora, N. 2023. Wasserstein barycenter for link prediction in temporal networks. *Journal of the Royal Statistical Society Series A: Statistics in Society*, 187(1): 180–208.
- Ucar, T. 2023. NESS: Node Embeddings from Static Sub-Graphs. *arXiv:2303.08958*.
- Vaswani, A.; Shazeer, N.; Parmar, N.; Uszkoreit, J.; Jones, L.; Gomez, A. N.; Kaiser, L.; and Polosukhin, I. 2023. Attention Is All You Need. *arXiv:1706.03762*.
- Veličković, P.; Cucurull, G.; Casanova, A.; Romero, A.; Liò, P.; and Bengio, Y. 2018. Graph Attention Networks. In *International Conference on Learning Representations*.
- Wang, P.; Xu, B.; Wu, Y.; and Zhou, X. 2014. Link Prediction in Social Networks: the State-of-the-Art. *CoRR*, abs/1411.5118.
- Yang, M.; Meng, Z.; and King, I. 2021. FeatureNorm: L2 Feature Normalization for Dynamic Graph Embedding. *CoRR*, abs/2103.00164.
- Yang, Z.; Ding, M.; Zhou, C.; Yang, H.; Zhou, J.; and Tang, J. 2020. Understanding Negative Sampling in Graph Representation Learning. In *Proceedings of the 26th ACM SIGKDD International Conference on Knowledge Discovery & Data Mining*, KDD '20, 1666–1676. New York, NY, USA: Association for Computing Machinery. ISBN 9781450379984.
- Yin, J.; Tang, M.; Cao, J.; You, M.; Wang, H.; and Alazab, M. 2023. Knowledge-Driven Cybersecurity Intelligence:

Software Vulnerability Coexploitation Behavior Discovery. *IEEE Transactions on Industrial Informatics*, 19(4): 5593–5601.

Zhang, C.; Zhang, H.; Yuan, D.; and Zhang, M. 2016. Deep learning based link prediction with social pattern and external attribute knowledge in bibliographic networks. In *2016 IEEE International Conference on Internet of Things (iThings) and IEEE Green Computing and Communications (GreenCom) and IEEE Cyber, Physical and Social Computing (CPSCom) and IEEE Smart Data (SmartData)*, 815–821. IEEE.

Zhang, M.; and Chen, Y. 2018. Link Prediction Based on Graph Neural Networks. In Bengio, S.; Wallach, H.; Larochelle, H.; Grauman, K.; Cesa-Bianchi, N.; and Garnett, R., eds., *Advances in Neural Information Processing Systems*, volume 31. Curran Associates, Inc.

Zhang, X.; He, Y.; Brugnone, N.; Perlmutter, M.; and Hirn, M. 2021. MagNet: a neural network for directed graphs. In *Proceedings of the 35th International Conference on Neural Information Processing Systems, NIPS '21*. Red Hook, NY, USA: Curran Associates Inc. ISBN 9781713845393.

Zhang, Z.; Cui, P.; and Zhu, W. 2022. Deep Learning on Graphs: A Survey. *IEEE Transactions on Knowledge and Data Engineering*, 34(1): 249–270.

Zhou, C.; Liu, Y.; Liu, X.; Liu, Z.; and Gao, J. 2017. Scalable Graph Embedding for Asymmetric Proximity. *Proceedings of the AAAI Conference on Artificial Intelligence*, 31(1).

Zhou, H.; Chegu, A.; Sohn, S. S.; Fu, Z.; de Melo, G.; and Kapadia, M. 2023. Harnessing Neighborhood Modeling and Asymmetry Preservation for Digraph Representation Learning. In Elkind, E., ed., *Proceedings of the Thirty-Second International Joint Conference on Artificial Intelligence, IJCAI-23*, 6519–6524. International Joint Conferences on Artificial Intelligence Organization. Sister Conferences Best Papers.

GravityGraphSAGE: Link Prediction in Directed Attributed Graphs

Technical Appendix

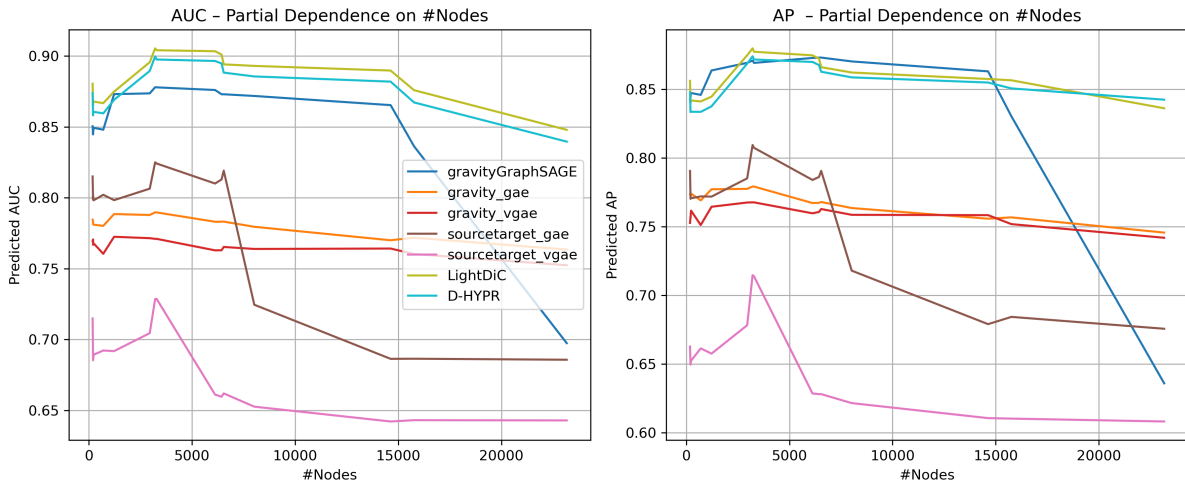


Figure 6: Random Forest Regression Partial Dependence Plot on the number of nodes in graphs.

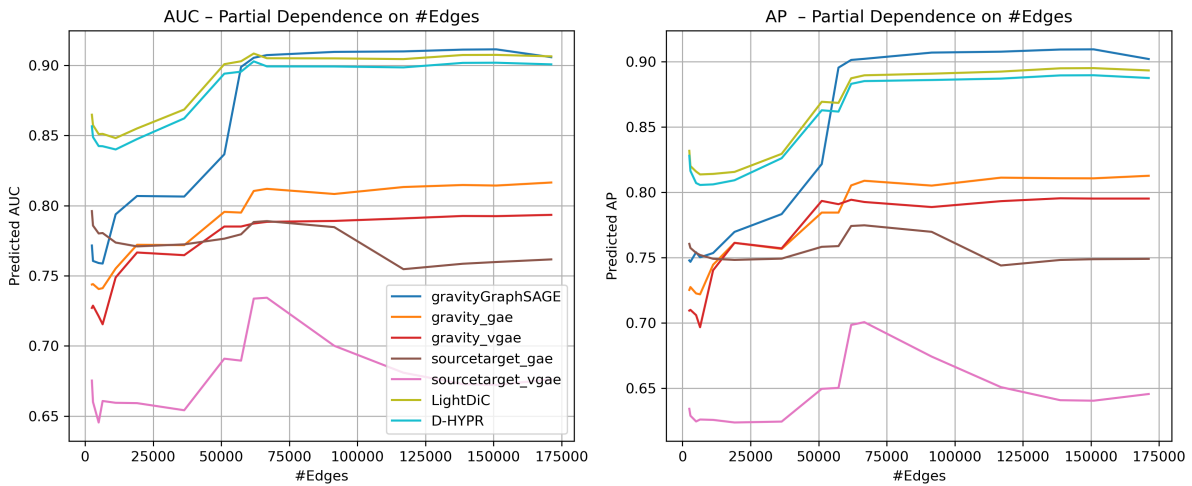


Figure 7: Random Forest Regression Partial Dependence Plot on the number of edges in graphs.

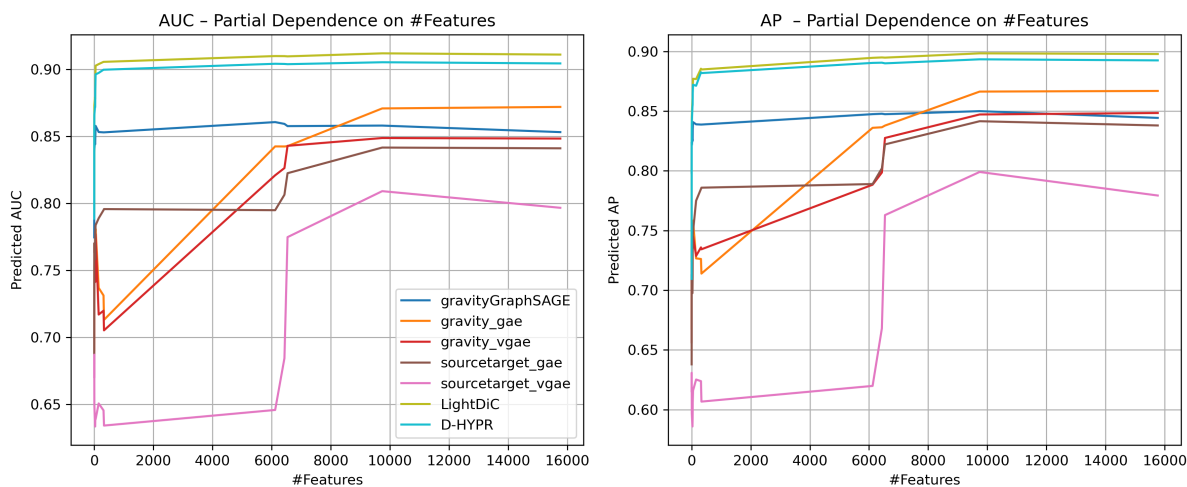


Figure 8: Random Forest Regression Partial Dependence Plot on the number of node features in graphs.

Table 5: Dataset Statistics. “*” indicates datasets comprising multiple networks; for these we select the network with the largest number of nodes.

Dataset	#Nodes	#Edges	#Features
Cora	2 708	5 429	1433
Citeseer	3 312	4 591	3 703
PubMed	19 717	88 651	500
foodweb_little_rock	183	2 494	37
cintestinalis	205	2 903	34
faculty_hiring*	206	4 988	332
messal_shale	700	6 444	152
un_migrations	232	11 228	28
polblogs	1 224	19 090	48
advogato	6 539	51 127	6 539
inplod	14 629	57 276	6
faculty_hiring-us*	3 284	61 936	3
openflights	3 214	66 771	9 740
cora-1998	23 166	91 500	1
caida_as*	8 020	36 406	1
fly_larva	2 952	116 922	316
jung	6 120	138 706	6 120
jdk	6 434	150 985	6 434
google	15 763	171 206	15 763

Dataset	Model	AUC (%)	AP (%)
advogato	GG-SAGE	84.11 ± 3.48	84.68 ± 3.55
	Gravity GAE	88.04 ± 0.24	88.79 ± 0.27
	Gravity VGAE	89.81 ± 0.03	90.21 ± 0.21
	Source/Target GAE	91.01 ± 0.12	90.61 ± 0.23
	Source/Target VGAE	87.84 ± 0.12	85.25 ± 0.19
	LightDiC	91.80 ± 0.20	91.30 ± 0.20
	D-HYPR	91.20 ± 1.00	90.70 ± 1.00
caida_as	GG-SAGE	78.56 ± 3.20	80.74 ± 2.81
	Gravity GAE	60.48 ± 0.82	56.12 ± 0.73
	Gravity VGAE	63.65 ± 0.91	59.47 ± 0.40
	Source/Target GAE	52.02 ± 2.88	50.82 ± 1.33
	Source/Target VGAE	52.38 ± 6.07	50.55 ± 4.50
	LightDiC	78.00 ± 0.20	65.00 ± 0.20
	D-HYPR	77.40 ± 1.00	64.80 ± 1.00
cintestinalis	GG-SAGE	70.90 ± 3.83	66.65 ± 4.02
	Gravity GAE	76.63 ± 0.62	75.11 ± 0.36
	Gravity VGAE	75.58 ± 0.33	75.81 ± 0.43
	Source/Target GAE	70.01 ± 6.02	64.57 ± 6.30
	Source/Target VGAE	54.92 ± 1.03	51.10 ± 1.25
	LightDiC	77.30 ± 0.20	75.90 ± 0.20
	D-HYPR	76.40 ± 1.00	75.00 ± 1.00
cora	GG-SAGE	48.67 ± 2.18	44.44 ± 0.98
	Gravity GAE	64.44 ± 0.13	61.04 ± 0.13
	Gravity VGAE	60.63 ± 0.46	55.11 ± 0.36
	Source/Target GAE	51.40 ± 1.97	47.66 ± 1.88
	Source/Target VGAE	55.52 ± 2.03	51.22 ± 1.54
	LightDiC	65.00 ± 0.20	62.60 ± 0.20
	D-HYPR	64.40 ± 1.00	62.00 ± 1.00
faculty_hiring	GG-SAGE	73.77 ± 1.91	77.38 ± 1.37
	Gravity GAE	60.96 ± 0.43	61.61 ± 0.94
	Gravity VGAE	61.45 ± 0.78	64.22 ± 1.27
	Source/Target GAE	83.45 ± 1.42	82.10 ± 1.33
	Source/Target VGAE	52.54 ± 10.03	53.56 ± 8.89
	LightDiC	84.00 ± 0.20	82.50 ± 0.20
	D-HYPR	83.40 ± 1.00	81.90 ± 1.00
faculty_hiring_us	GG-SAGE	95.93 ± 0.43	94.95 ± 0.31
	Gravity GAE	83.28 ± 0.63	82.79 ± 0.65
	Gravity VGAE	76.32 ± 2.60	80.17 ± 1.11
	Source/Target GAE	95.97 ± 0.05	93.60 ± 0.16
	Source/Target VGAE	94.31 ± 0.90	89.62 ± 2.43
	LightDiC	96.40 ± 0.20	94.70 ± 0.20
	D-HYPR	95.80 ± 1.00	94.20 ± 1.00
fly_larva	GG-SAGE	93.64 ± 0.56	93.28 ± 0.56
	Gravity GAE	79.59 ± 0.42	79.98 ± 0.48
	Gravity VGAE	79.55 ± 0.55	79.72 ± 0.50
	Source/Target GAE	78.90 ± 0.79	77.43 ± 0.38
	Source/Target VGAE	68.23 ± 2.90	67.47 ± 3.47
	LightDiC	92.50 ± 0.20	92.60 ± 0.20
	D-HYPR	91.90 ± 1.00	91.90 ± 1.00
foodweb_little_rock	GG-SAGE	83.81 ± 1.63	79.43 ± 1.70
	Gravity GAE	75.86 ± 5.88	69.44 ± 5.47
	Gravity VGAE	72.48 ± 1.62	63.32 ± 1.11
	Source/Target GAE	95.28 ± 0.16	92.81 ± 0.38
	Source/Target VGAE	79.18 ± 1.30	69.13 ± 1.20
	LightDiC	95.80 ± 0.20	93.30 ± 0.20
	D-HYPR	95.40 ± 1.00	92.90 ± 1.00
google	GG-SAGE	88.79 ± 1.29	89.14 ± 0.66
	Gravity GAE	92.46 ± 0.52	92.49 ± 0.59
	Gravity VGAE	88.22 ± 0.86	90.34 ± 0.79
	Source/Target GAE	81.59 ± 0.84	81.39 ± 0.60
	Source/Target VGAE	72.56 ± 5.57	70.16 ± 6.11
	LightDiC	93.00 ± 0.20	93.00 ± 0.20
	D-HYPR	92.40 ± 1.00	92.50 ± 1.00
inplod	GG-SAGE	92.92 ± 2.05	92.96 ± 2.30
	Gravity GAE	74.48 ± 0.81	73.43 ± 1.21
	Gravity VGAE	77.05 ± 0.45	78.67 ± 0.59
	Source/Target GAE	58.52 ± 5.00	53.07 ± 4.39
	Source/Target VGAE	55.81 ± 1.62	49.85 ± 1.12
	LightDiC	92.00 ± 0.20	88.80 ± 0.20
	D-HYPR	91.20 ± 1.00	88.20 ± 1.00
jdk	GG-SAGE	97.47 ± 0.38	96.62 ± 0.67
	Gravity GAE	87.59 ± 0.65	87.17 ± 1.88
	Gravity VGAE	84.50 ± 0.40	81.99 ± 0.26
	Source/Target GAE	78.15 ± 1.37	78.87 ± 1.00
	Source/Target VGAE	58.04 ± 10.99	56.28 ± 13.20
	LightDiC	96.50 ± 0.20	96.00 ± 0.20
	D-HYPR	95.90 ± 1.00	95.50 ± 1.00
jung	GG-SAGE	97.03 ± 1.27	96.07 ± 1.71
	Gravity GAE	87.93 ± 0.34	87.50 ± 1.55
	Gravity VGAE	85.02 ± 0.18	82.48 ± 0.22
	Source/Target GAE	75.88 ± 2.19	77.61 ± 1.11
	Source/Target VGAE	59.51 ± 10.40	57.10 ± 13.52
	LightDiC	96.00 ± 0.20	95.40 ± 0.20
	D-HYPR	95.60 ± 1.00	95.00 ± 1.00
messal_shale	GG-SAGE	73.38 ± 6.44	74.91 ± 6.04
	Gravity GAE	62.67 ± 6.78	60.43 ± 4.19
	Gravity VGAE	52.57 ± 0.60	54.56 ± 1.00
	Source/Target GAE	84.04 ± 0.71	79.66 ± 1.06
	Source/Target VGAE	69.06 ± 4.57	64.83 ± 2.50
	LightDiC	84.30 ± 0.20	79.80 ± 0.20
	D-HYPR	83.20 ± 1.00	78.70 ± 1.00
openflights	GG-SAGE	98.01 ± 0.51	98.52 ± 0.26
	Gravity GAE	95.09 ± 0.23	94.93 ± 0.22
	Gravity VGAE	93.77 ± 0.22	94.52 ± 0.15
	Source/Target GAE	96.78 ± 0.11	96.53 ± 0.14
	Source/Target VGAE	94.01 ± 0.56	93.29 ± 0.50
	LightDiC	97.50 ± 0.20	97.90 ± 0.20
	D-HYPR	97.00 ± 1.00	97.40 ± 1.00
polblogs	GG-SAGE	90.09 ± 0.55	83.76 ± 0.34
	Gravity GAE	83.84 ± 0.28	81.77 ± 0.81
	Gravity VGAE	84.14 ± 0.22	83.09 ± 0.72
	Source/Target GAE	77.48 ± 2.17	73.01 ± 2.16
	Source/Target VGAE	60.56 ± 1.30	57.80 ± 2.72
	LightDiC	88.50 ± 0.20	83.10 ± 0.20
	D-HYPR	87.80 ± 1.00	82.50 ± 1.00
un_migrations	GG-SAGE	82.29 ± 0.96	75.68 ± 0.92
	Gravity GAE	75.97 ± 0.50	77.05 ± 0.55
	Gravity VGAE	75.62 ± 0.38	76.48 ± 0.63
	Source/Target GAE	72.16 ± 8.47	65.61 ± 8.27
	Source/Target VGAE	62.13 ± 1.17	55.25 ± 1.76
	LightDiC	81.80 ± 0.20	77.40 ± 0.20
	D-HYPR	81.00 ± 1.00	76.80 ± 1.00

Table 6: Performance of models on selected Netzschleuder datasets. Best results are highlighted in green and in bold are indicated comparable performances.